

We are IntechOpen, the world's leading publisher of Open Access books Built by scientists, for scientists

6,900

Open access books available

186,000

International authors and editors

200M

Downloads

Our authors are among the

154

Countries delivered to

TOP 1%

most cited scientists

12.2%

Contributors from top 500 universities



WEB OF SCIENCE™

Selection of our books indexed in the Book Citation Index
in Web of Science™ Core Collection (BKCI)

Interested in publishing with us?
Contact book.department@intechopen.com

Numbers displayed above are based on latest data collected.
For more information visit www.intechopen.com



Transient Responses on Traveling-Wave Loop Directional Filters

Kazuhito Murakami

Additional information is available at the end of the chapter

<http://dx.doi.org/10.5772/50459>

1. Introduction

In design consideration of microwave and millimeter-wave planar circuits, efficient simulation tools have been required for visualizing the operation characteristics of passive circuit components. Also, to clarify the signal propagation in the circuit system is very important in terms of engineering and educational effects. Microwave simulators are widely used as the supporting tool of microwave circuit design and development. For analyzing the circuit components on planar circuits, several numerical techniques are described about the 3-D electromagnetic field analysis modeling [1]. Nowadays, the method of moments (MoM) [2] and the finite-difference time-domain method (FDTD) [3],[4] are mostly used among microwave engineers, and the SNAP simulator [10] is SPICE like one. On the other hand, there are various microwave circuit components using parallel coupled lines and loop resonators [5]. A square loop line with parallel coupled lines is used as ring resonators and traveling-wave loop directional filters. Here, in order to solve the transient problem of the microwave circuit components composed of transmission lines, we provide a numerical analysis method introduced systematic mixed even and odd modes modeling for coupled lines. This method based on a modified central difference method [8] can be applied to the time domain analysis of the microwave circuit components constructed with the parallel tightly coupled lines. For ring resonators and traveling-wave loop directional filters composed of such components [6],[7], to clarify the circuit operation, the transient behavior of the voltage and current waves of transmission line networks will be represented with dynamic expressions. In order to elucidate the mechanism of the circuit operation, the behavior of propagating signals on the transmission line network has been represented in [9]. In this article, we describe the utilization of the modified central difference method incorporating internal boundary treatments. Using this simulation technique, the time and frequency domain properties of the ring resonator and traveling-wave multi-loop directional coupler filters are analyzed and demonstrated.

For obtaining accurate operation characteristics of circuit components, simulation techniques with processing multiple reflections are required. The transient behavior of the voltage and current waves on the ring resonator and traveling-wave loop directional filters is demonstrated to obtain the power division and isolation properties of the directional couplers by using a numerical analysis model. The represented transient phenomena include the effects of multiple reflection waves caused by line discontinuities and parallel coupling. The operating mechanism of the circuit components can be easily confirmed by the visualization of the computed voltage and current solutions. The transient responses along the transmission lines are represented with the variations of the instantaneous voltage and current distributions including all the multiple reflections. Additionally, using the input and output responses extracted from the voltage and current solutions for a Gaussian pulse excitation, the frequency responses are obtained by using the fast Fourier transform.

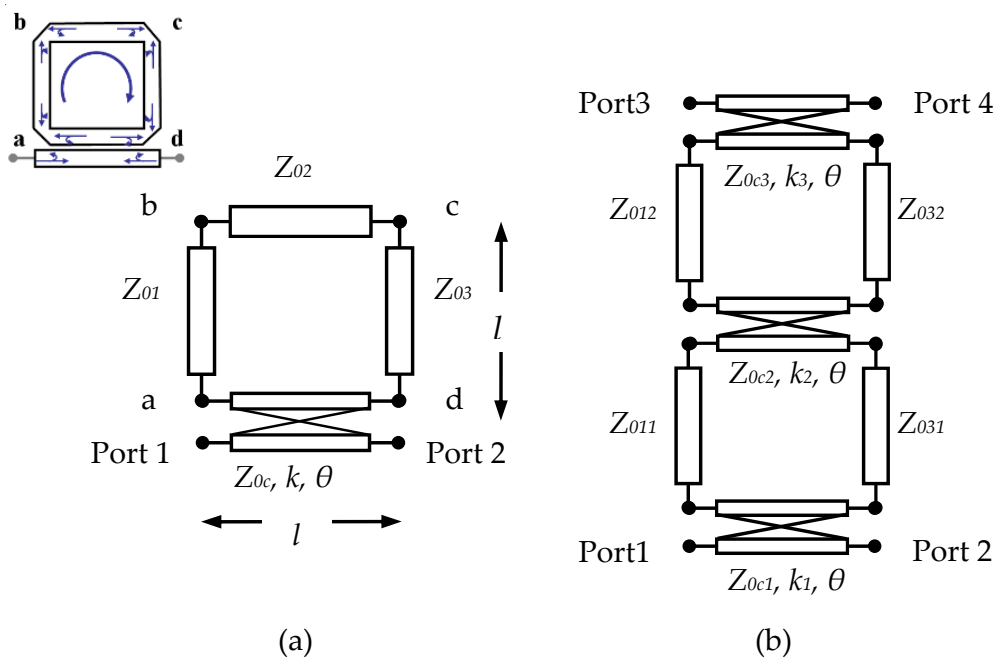


Figure 1. (a) A ring resonator and (b) traveling-wave loop directional filter.

2. Modeling

2.1. Modeling of a single transmission line

The configuration of a ring resonator and traveling-wave loop directional filter is shown in Figure 1. By applying numerical even- and odd-mode analysis model to parts of parallel coupled lines, the solution of the whole system can be solved by single transmission line analysis, with the assumption of TEM mode propagation. The 1-D modeling of the single transmission line has reported in [8]. Telegrapher's equations can be generally written by

$$\frac{\partial}{\partial x} \begin{bmatrix} V(x,t) \\ I(x,t) \end{bmatrix} + \begin{bmatrix} 0 & L \\ C & 0 \end{bmatrix} \frac{\partial}{\partial t} \begin{bmatrix} V(x,t) \\ I(x,t) \end{bmatrix} = - \begin{bmatrix} 0 & R \\ G & 0 \end{bmatrix} \begin{bmatrix} V(x,t) \\ I(x,t) \end{bmatrix} \quad (1)$$

where $V(x,t)$, $I(x,t)$ are the line voltage and current at any time t and at distance x , respectively. L , R , C and G are the inductance, resistance, capacitance and conductance per unit length of the line, respectively. According to the above assumption, the characteristic impedance and phase velocity of the secondary constant parameters are described by $Z_0 = \sqrt{L/C}$ and $v_p = 1/\sqrt{LC}$, respectively. To solve the transmission line equations, the modified central difference approximation is applied to (1). The difference equations can be described as follows:

$$\frac{1}{2\Delta x} \begin{bmatrix} V_{i+1,j} - V_{i-1,j} \\ I_{i+1,j} - I_{i-1,j} \end{bmatrix} + \begin{bmatrix} 0 & -L \\ C & 0 \end{bmatrix} \frac{1}{2\Delta t} \begin{bmatrix} 2V_{i,j+1} - (V_{i+1,j} + V_{i-1,j}) \\ 2I_{i,j+1} - (I_{i+1,j} + I_{i-1,j}) \end{bmatrix} = - \begin{bmatrix} 0 & R \\ G & 0 \end{bmatrix} \frac{1}{2} \begin{bmatrix} V_{i+1,j} + V_{i-1,j} \\ I_{i+1,j} + I_{i-1,j} \end{bmatrix} \quad (2)$$

The derived update equations in the case of lossless line are as follows:

$$\begin{bmatrix} V_{i,j+1} \\ I_{i,j+1} \end{bmatrix} = \frac{1}{2} \begin{bmatrix} 1 & Z_0 \\ 1/Z_0 & 1 \end{bmatrix} \begin{bmatrix} V_{i-1,j} \\ I_{i-1,j} \end{bmatrix} + \frac{1}{2} \begin{bmatrix} 1 & -Z_0 \\ -1/Z_0 & 1 \end{bmatrix} \begin{bmatrix} V_{i+1,j} \\ I_{i+1,j} \end{bmatrix} \quad (3)$$

where the suffices $i,j,i+1,i-1$, etc. denote the position at $i=i\Delta x$ ($0 < i \leq l$), $j=j\Delta t$ ($\Delta t = \Delta x/v_p$) on the $(x-t)$ plane. l is the line length.

2.2. Modeling of coupled transmission lines

Here, as shown in Figure 2, we carry out the even- and odd-mode numerical analysis for the parts of the coupled lines in Figure 1. In the considered parallel coupled lines model, Z_{0e} and Z_{0o} , respectively, are the even- and odd-mode equivalent impedances decided as follows:

$$Z_{0e} = Z_{0c} \sqrt{(1+k)/(1-k)} \quad (4)$$

$$Z_{0o} = Z_{0c} \sqrt{(1-k)/(1+k)} \quad (5)$$

where Z_{0c} and k are the characteristic impedance and coupling coefficient, respectively. The line voltages and currents for each equivalent impedance line are obtained by using (3).

2.3. Boundary treatments

In this modeling, the boundary treatments of both the sides of the coupled line need to calculate at each of time step. For the voltages and currents at the boundaries of the coupled line part as shown in Figure 3, the following scattering matrices expressed by the reflection coefficient are used to compute the reflected and transmitted quantities.

$$\begin{bmatrix} V_{p1}^- \\ V_{p3}^- \\ V_{ea}^- \\ V_{oa}^- \end{bmatrix} = \begin{bmatrix} 0 & \Gamma_a & (1-\Gamma_a)/2 & (1+\Gamma_a)/2 \\ \Gamma_a & 0 & (1-\Gamma_a)/2 & -(1+\Gamma_a)/2 \\ (1+\Gamma_a) & (1+\Gamma_a) & -\Gamma_a & 0 \\ (1-\Gamma_a) & -(1-\Gamma_a) & 0 & \Gamma_a \end{bmatrix} \begin{bmatrix} V_{p1}^+ \\ V_{p3}^+ \\ V_{ea}^+ \\ V_{oa}^+ \end{bmatrix} \quad (6)$$

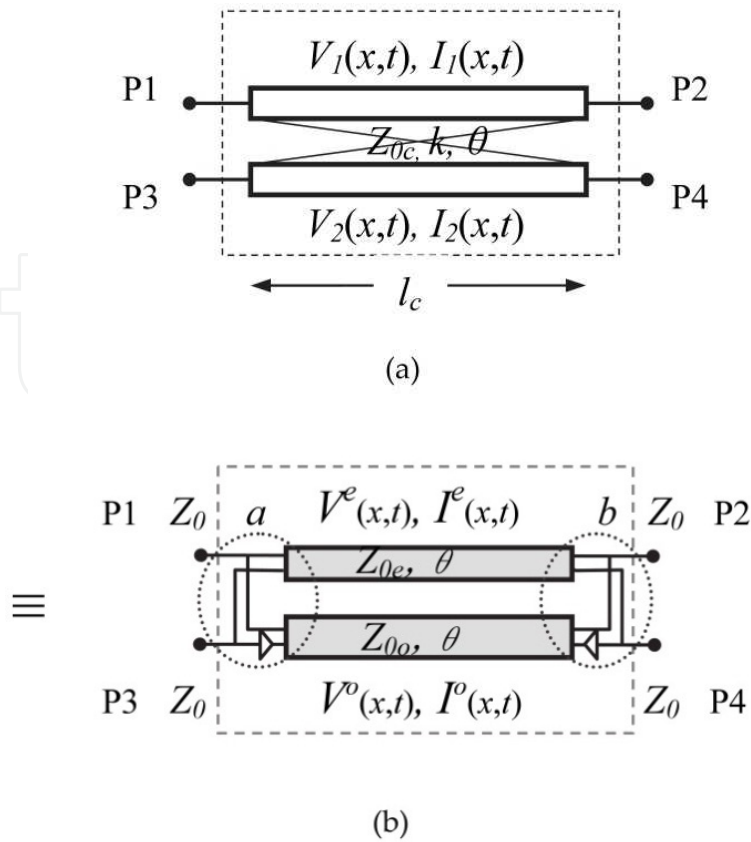


Figure 2. An equivalent circuit model of a basic coupled line.

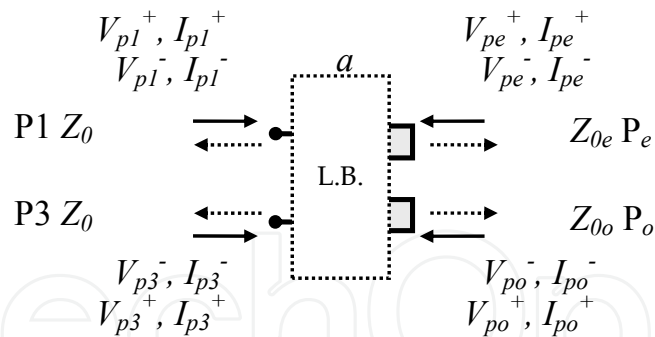


Figure 3. Four ports boundary at left side discontinuity of Figure 2 (b)

$$\begin{bmatrix} I_{p1}^- \\ I_{p3}^- \\ I_{ea}^- \\ I_{oa}^- \end{bmatrix} = \begin{bmatrix} 0 & -\Gamma_a & -(1+\Gamma_a)/2 & -(1-\Gamma_a)/2 \\ -\Gamma_a & 0 & -(1+\Gamma_a)/2 & (1-\Gamma_a)/2 \\ (1-\Gamma_a) & (1-\Gamma_a) & -\Gamma_a & 0 \\ (1+\Gamma_a) & -(1+\Gamma_a) & 0 & \Gamma_a \end{bmatrix} \begin{bmatrix} I_{p1}^+ \\ I_{p3}^+ \\ I_{ea}^+ \\ I_{oa}^+ \end{bmatrix} \tag{7}$$

where V_{pi}^+ , V_{pi}^- , I_{pi}^+ , I_{pi}^- ($i=1, 3, e, o$) denote the incident and reflected voltages, and currents from each line at the left side discontinuity, and the reflection coefficient is

$$\Gamma_a = (Z_{0e} - Z_{0c}) / (Z_{0e} + Z_{0c}) = -(Z_{0o} - Z_{0c}) / (Z_{0o} + Z_{0c}) \quad (8)$$

Similarly, be done to the right side one. Further, the boundary treatments for each port of the coupled lines with mismatched load are carried out as follows:

$$V_{pk}^+ = \Gamma_k V_{pk}^+ + (1 + \Gamma_k) V_{pk}^- \quad (9)$$

$$I_{pk}^+ = -\Gamma_k I_{pk}^+ - (1 - \Gamma_k) I_{pk}^- \quad (10)$$

where $\Gamma_k = (Z_{pk} - Z_{0c}) / (Z_{pk} + Z_{0c})$, ($k=1$ to 4). These boundary treatments need to be performed at each time step.

Here, the initial conditions of each transmission line are given as follows: $V^e(x, t=0)=0$, $I^e(x, t=0)=0$ and $V^o(x, t=0)=0$, $I^o(x, t=0)=0$. Then, for Port1 excitation, the boundary conditions at each port of the circuit component are also given as follows: $V_{port1}(t) = e(t)Z_0 / (Z_s + Z_0)$, $I_{port1}(t) = V_{port1}(t) / Z_0$, $V_{port2}(t)=0$, $I_{port2}(t)=0$, $V_{port3}(t)=0$, $I_{port3}(t)=0$, $V_{port4}(t)=0$ and $I_{port4}(t)=0$. The obtained voltage and current solutions of the ring resonator and traveling-wave loop directional filters are demonstrated dynamically.

As a final processing, the line voltage and current solutions of the coupled transmission lines are numerically computed by the following equations.

$$V_1(x, t) = (V^e(x, t) + V^o(x, t)) / 2 \quad (11)$$

$$I_1(x, t) = (I^e(x, t) + I^o(x, t)) / 2 \quad (12)$$

$$V_2(x, t) = (V^e(x, t) - V^o(x, t)) / 2 \quad (13)$$

$$I_2(x, t) = (I^e(x, t) - I^o(x, t)) / 2 \quad (14)$$

where $V^e(x, t)$, $V^o(x, t)$ and $I^e(x, t)$, $I^o(x, t)$ are the even- and odd-mode line voltages, and currents, respectively.

Algorithm

Preprocessing: Decision of line parameters

Step 1. Set initial values

$$V(x, t=0), I(x, t=0): 0 < x < l$$

Step 2. $t = t + \Delta t$ if $t > t_n$ then exit

Step 3. Calculate update equations

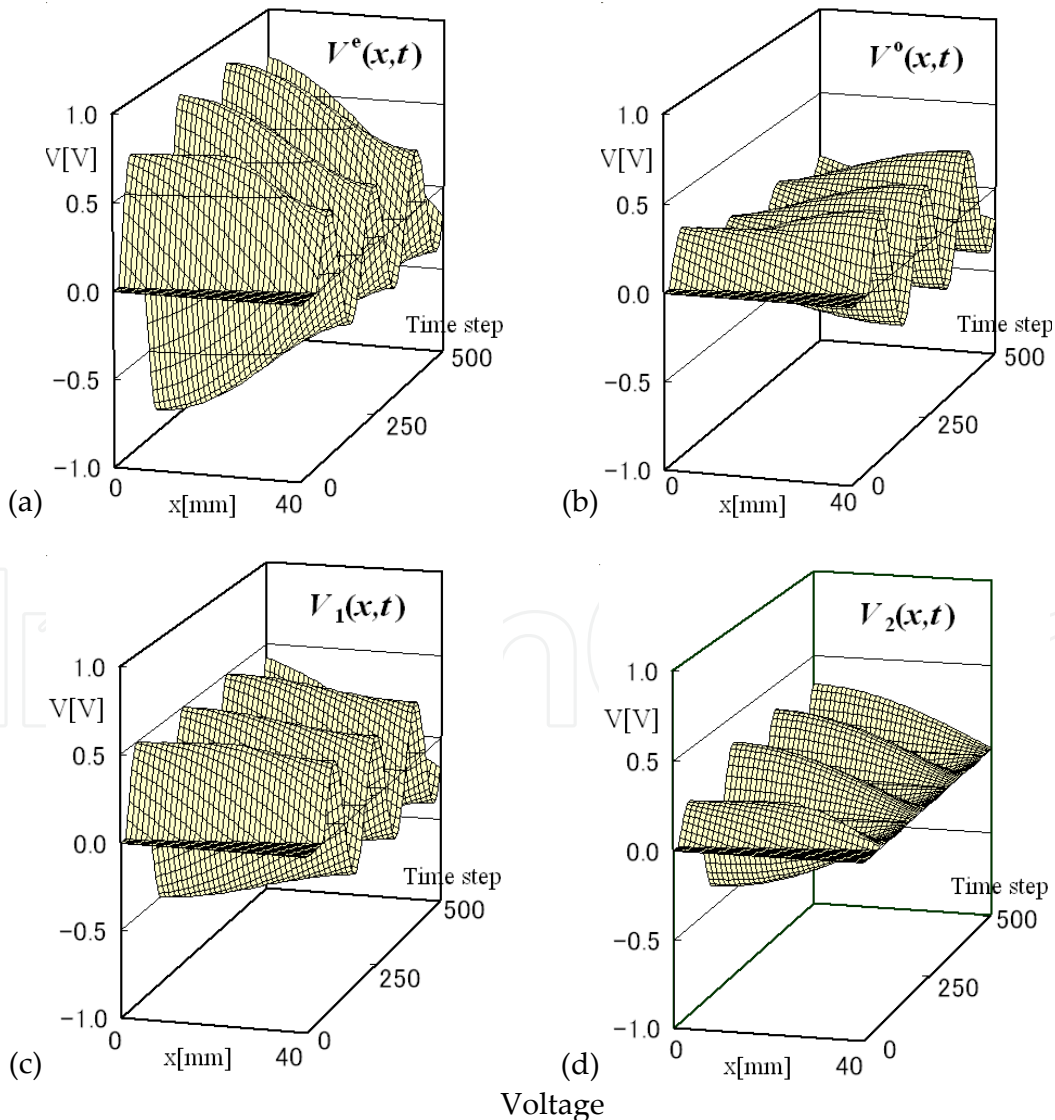
$$V(x, t), I(x, t): 0 < x < l$$

Step 4. Boundary treatments

Step 5. Go to Step2

Postprocessing: Visualization of results

The solutions of the basic coupled lines as shown in Figure 2 are computed by the numerical even and odd modes analysis. The voltage and current solutions of the equivalent even- and odd-mode impedance lines of uniform parallel coupled lines are shown in Figure 4 (a)(b)(e)(f). Consequently, by synthesizing these solutions, namely using equations (11)-(14), the solutions for the drive line and sense line are obtained as shown in Figure 4 (c)(d)(g)(h). Subsequently, Figure 5 and Figure 6 show the input and output voltage waveforms extracted from the voltage solutions of the basic coupled lines with and without matched loads, respectively, from 0 to 800 time steps. The used design parameters as follows: $Z_0=50\Omega$, $Z_{0e}=50\Omega$, $k=0.707$, $Z_{0o}=120\Omega$, $Z_{0o}=20.8\Omega$, $l_c=40\text{mm}$, $\Delta x=1\text{mm}$, $\Delta t=3.33\text{ps}$, $\epsilon_r=1$, for $e_r=\sin(2\pi f t)$: $f_c=1.875\text{GHz}$).



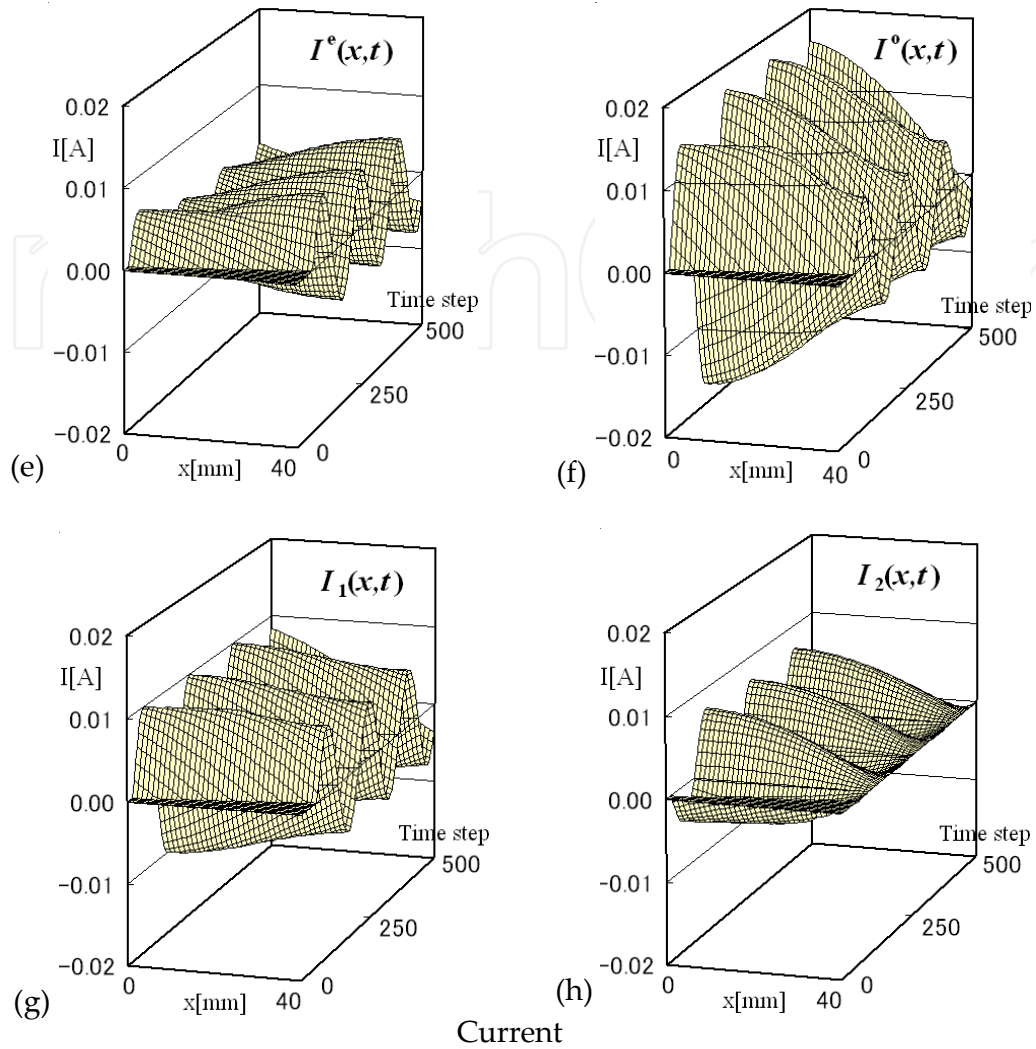


Figure 4. Transient solutions of the even-mode and odd-mode equivalent lines and the solution of the basic coupled line synthesized with their solutions: Voltage (upper) and Current (lower).

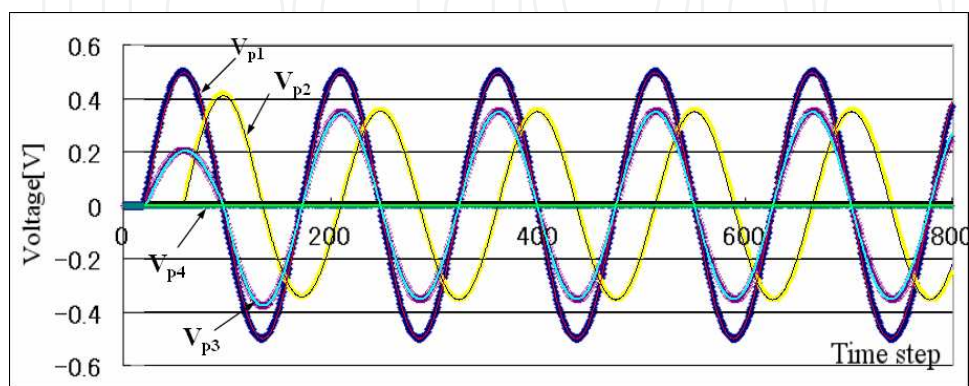


Figure 5. Input and output responses of the basic coupled lines with matched loads: MCD (dotted line) and SNAP (solid line). ($Z_0=50\Omega$, $Z_{0c}=50\Omega$, $k=0.707$, $l_c=40\text{mm}$).

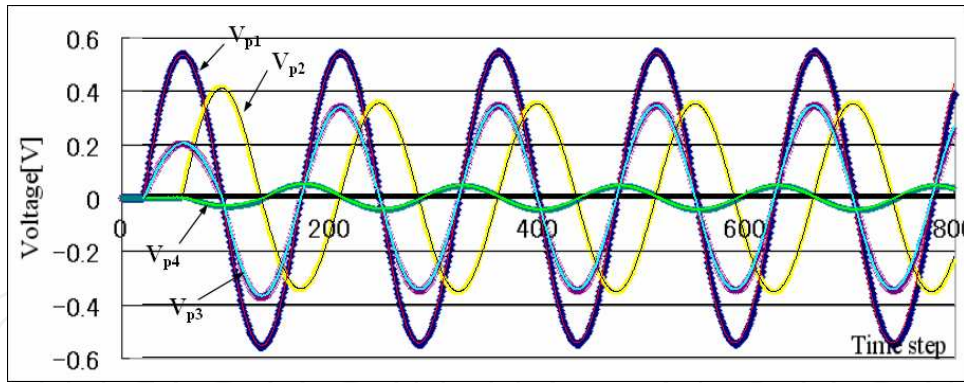


Figure 6. Input and output responses of the basic coupled lines with mismatched loads: MCD (dotted line) and SNAP (solid line). ($Z_0=50\Omega$, $Z_{0c}=60\Omega$, $k=0.707$, $l_c=40\text{mm}$).

3. Wave propagation in the transmission line networks

In this section, several simulation results are shown for representing the wave propagation along the transmission line network. The transient voltage and current responses of the ring resonator and traveling-wave multi-loop directional coupler filters are analyzed and demonstrated with the time domain analysis.

3.1. Transient behavior of ring resonator filter

First, it is shown that the transient voltage and current responses of the ring resonator filter in Figure 1 (a) are demonstrated in the time domain. The designed parameters for this band stop filter (BSF) were used as follows: $Z_0=50\Omega$, $Z_{01}=Z_{03}=55\Omega$, $Z_{02}=35.4\Omega$, $Z_{0e}=130\Omega$, $Z_{0o}=40.9\Omega$, $l=40\text{mm}$, $\Delta x=1\text{mm}$, $\Delta t=3.33\text{ps}$, $\epsilon_r=1$, for a sinusoidal wave ($e_i=\sin(2\pi f_c t)$: f_c center frequency 1.875GHz) excitation. The variations of the instantaneous voltage and current distributions of the transmission line in the transient region are represented by the dynamic expression as shown in Figure 7. Also, Figure 8 shows the voltage and current distributions at steady state after 5000 time steps, to represent the standing wave at the center frequency. This figure represents the difference of the resonance phenomena in loop line between BSF and all-pass ring resonator. Figure 9 shows the input and output responses, in which the transmission zero and full-pass into port 2, respectively, are observed. In the case of the BSF, from the observed responses, it considerably takes much more CPU time up to steady state region. The designed parameters for the case of all-pass were used as follows: $Z_0=50\Omega$, $Z_{01}=Z_{03}=50\Omega$, $Z_{02}=50\Omega$, $Z_{0e}=120.7\Omega$, $Z_{0o}=20.8\Omega$, $l=40\text{mm}$, $\Delta x=1\text{mm}$, $\Delta t=3.33\text{ps}$, $\epsilon_r=1$.

3.2. Time responses of traveling-wave multi-loop directional filters

Next, we show the time responses for the traveling-wave double-loop 3dB directional coupler as shown in Figure 1 (b). Figure 10 shows the variation of instantaneous voltage and current distributions on the directional coupler in the steady state after 1500 time steps. The isolation at port 4 and the equal power division into ports 2 and 3 are observed for the 3-dB coupler at the center frequency. Note that the envelope denotes the standing waves on the transmission lines, in which they appear at only the coupled line area. In Figure 11, the input and output

voltage waveforms at each port are represented for 2000 time steps. The CPU time took in a few seconds. The following designed parameters were used: $Z_0=50\Omega$, $Z_{011}=Z_{031}=Z_{012}=Z_{032}=50\Omega$, $Z_{0e1}=Z_{0e2}=Z_{0e3}=120.7\Omega$, $Z_{0o1}=Z_{0o2}=Z_{0o3}=20.8\Omega$, $l=40\text{mm}$, $\Delta x=1\text{mm}$, $\Delta t=3.33\text{ps}$, $\epsilon_r=1$ at $f_c=1.875\text{GHz}$.

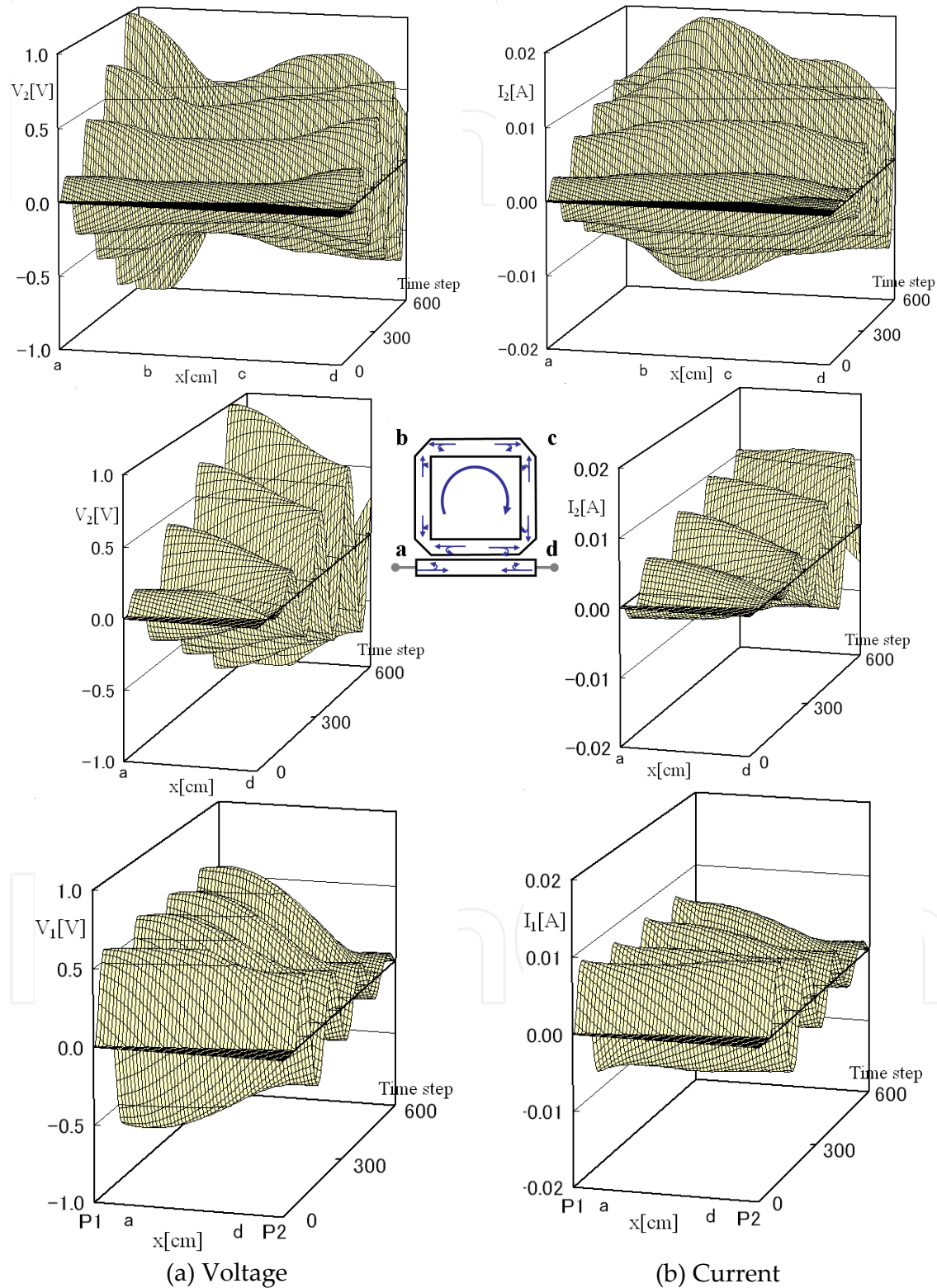


Figure 7. Transient behaviors of voltage and current on the ring resonator BSF from 0 to 600 time steps.

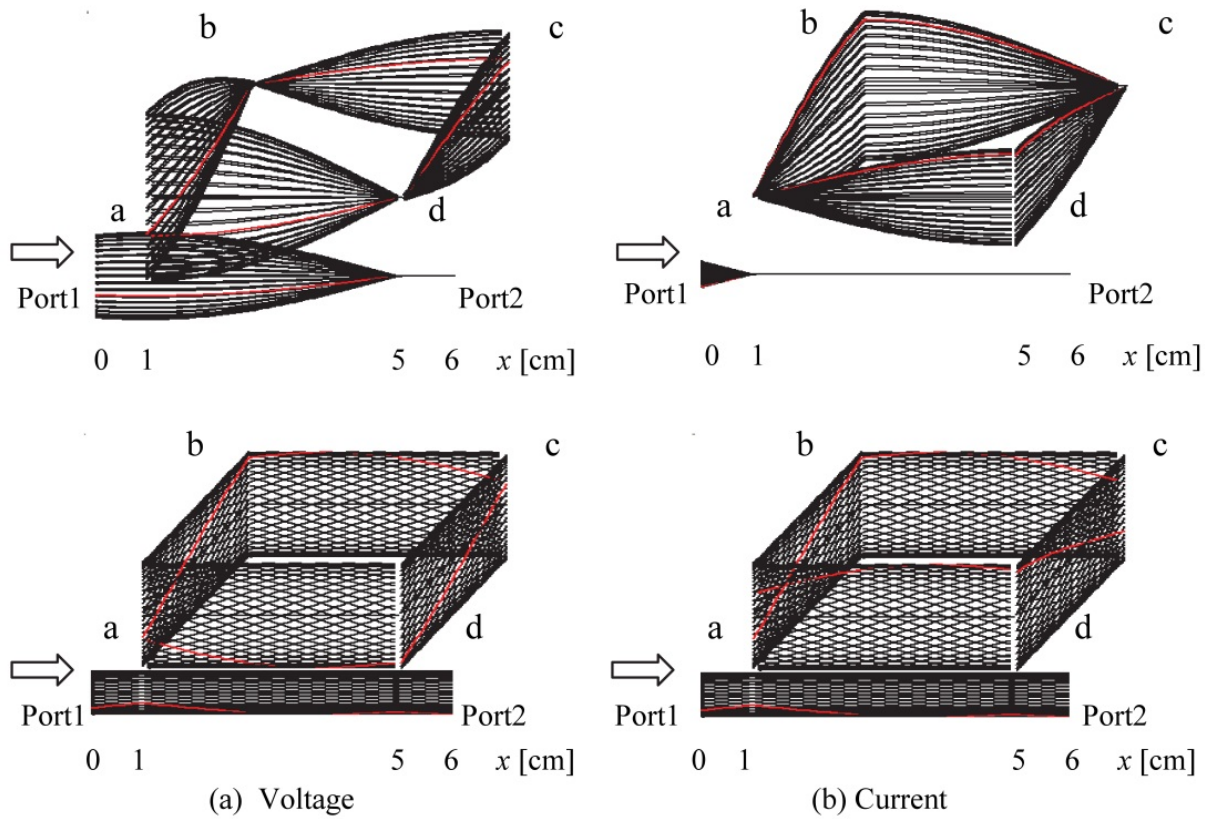


Figure 8. Variation of instantaneous voltage and current distributions on the ring resonator BSF (upper) and all-pass (lower) at steady state after 5000 time steps. Red lines denote a snapshot of the plot.

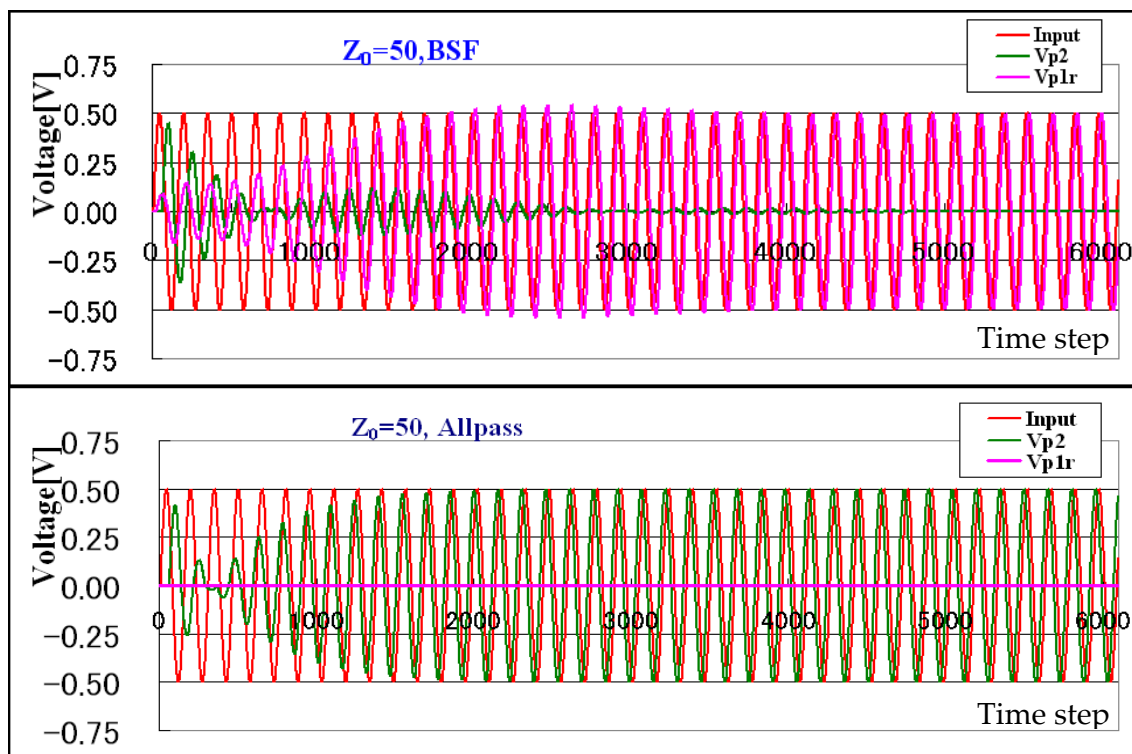


Figure 9. Input and output voltage waveforms of the ring resonator BSF (upper) and all-pass (lower) from 0 to 6000 time steps.

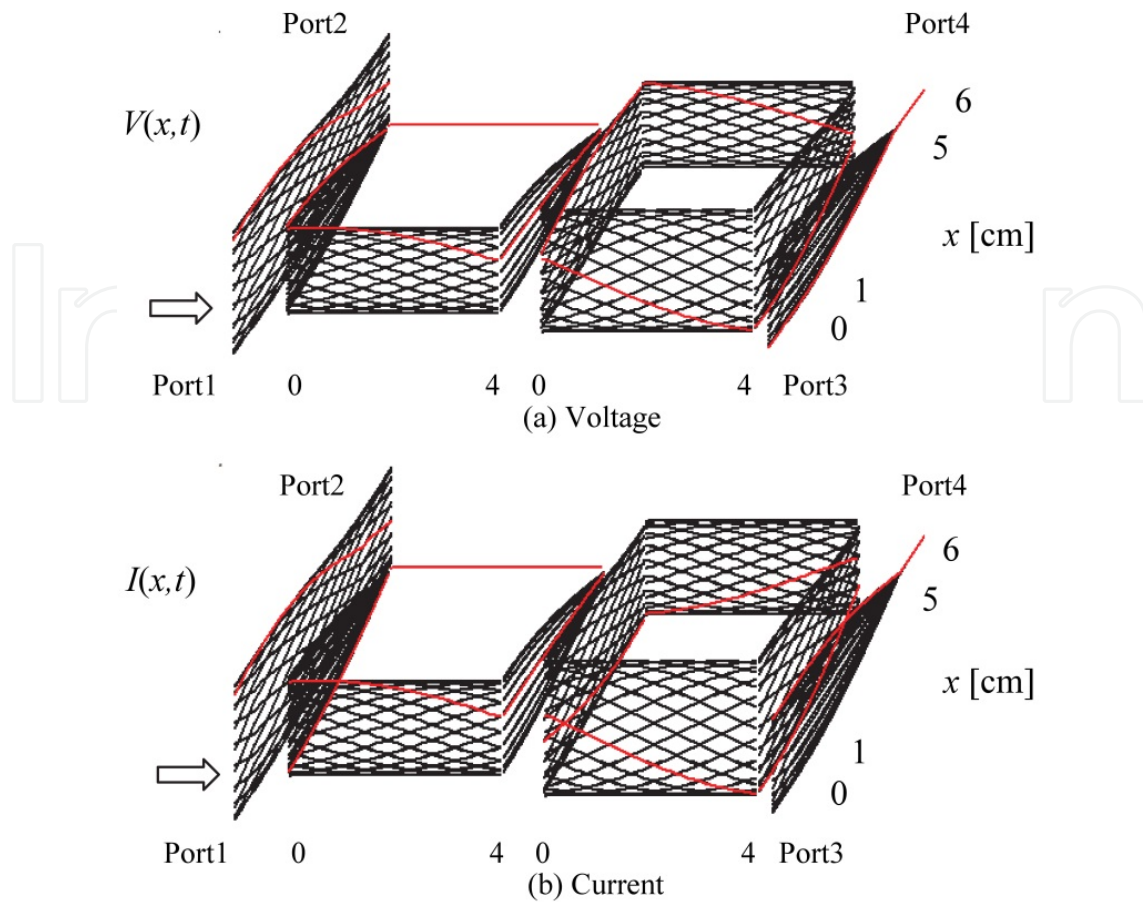


Figure 10. Variation of the instantaneous voltage and current distributions on the double-loop 3-dB directional coupler after 1500 time steps. Red lines denote a snapshot of the plot.

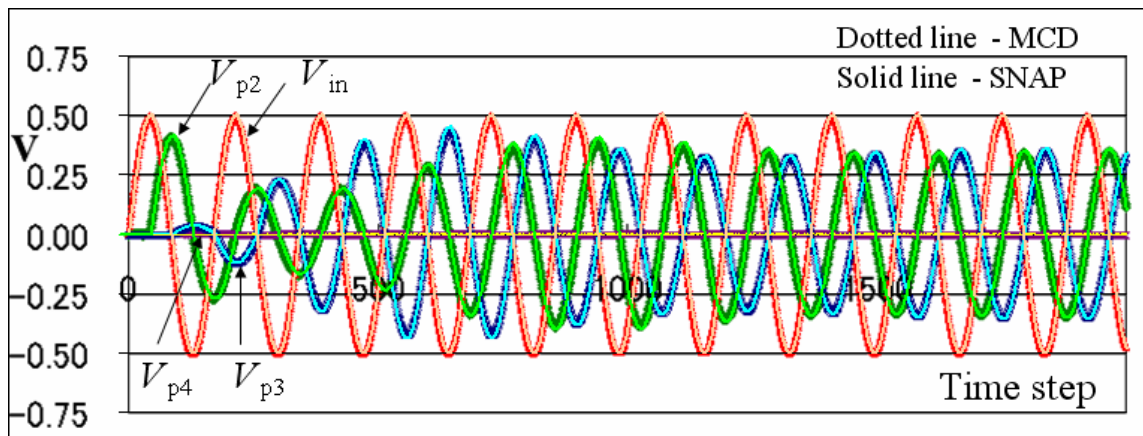


Figure 11. Input and output voltage waveforms of the double-loop directional coupler for sinusoidal wave excitation at the center frequency.

Figure 12 shows the time responses for the traveling-wave triple-loop directional filter. The variation of instantaneous voltage and current distributions on the directional filter in the steady state are illustrated after 3000 time steps. The isolation at ports 4 and 2, and full power into port 3 is observed for the directional filter at the center frequency f_c . The input and output voltage waveforms at each port for 4000 time steps are represented in Figure 13.

Additionally, at dual frequencies f_a and f_b , near equal power division into ports 2 and 3 are represented. The following parameters were used: $Z_0=50\Omega$, $Z_{011}=Z_{031}=Z_{012}=Z_{032}=Z_{013}=Z_{033}=50\Omega$, $Z_{0e1}=Z_{0e2}=Z_{0e3}=Z_{0e4}=120.7\Omega$, $Z_{0o1}=Z_{0o2}=Z_{0o3}=Z_{0o4}=20.8\Omega$, $l=40\text{mm}$, $\Delta x=1\text{mm}$, $\Delta t=3.33\text{ps}$, $\epsilon_r=1$ at $f_c=1.875\text{GHz}$.

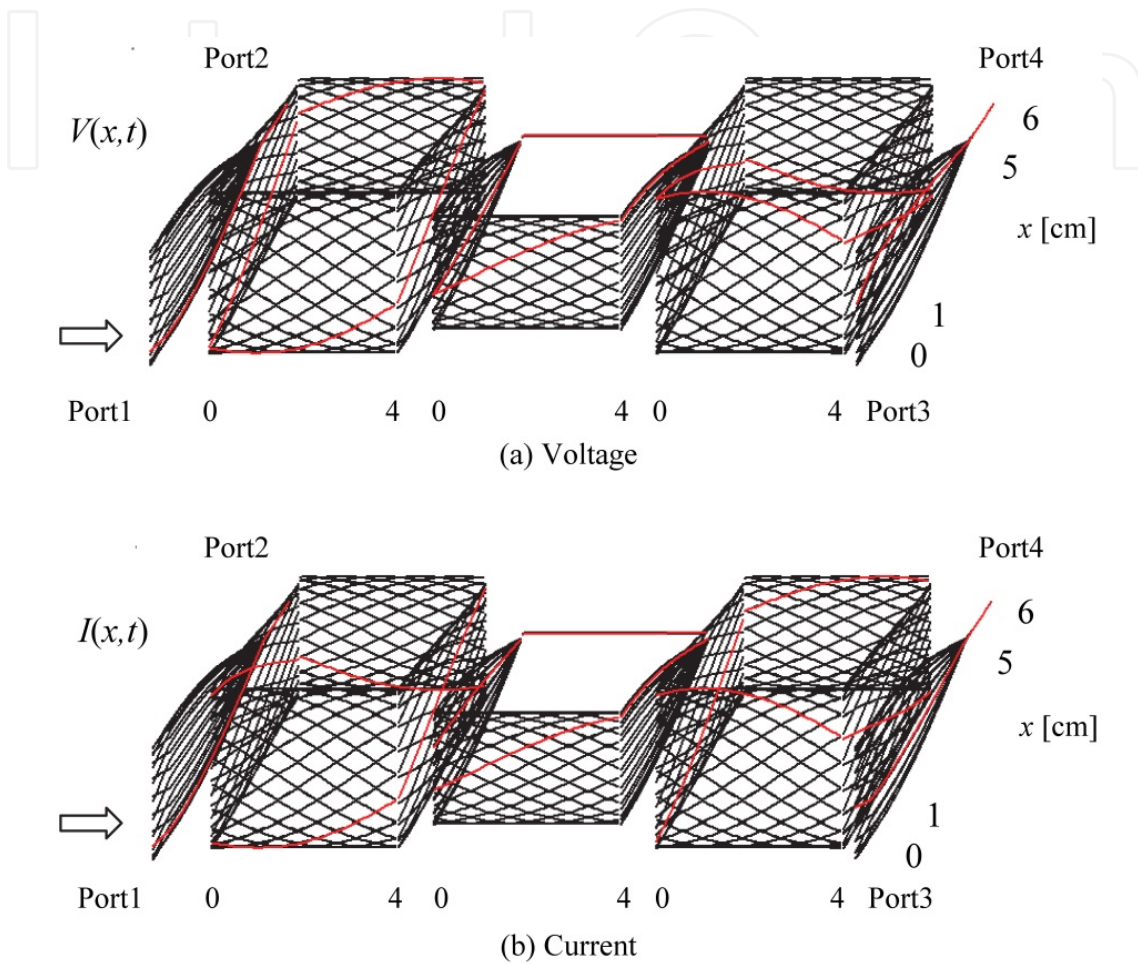
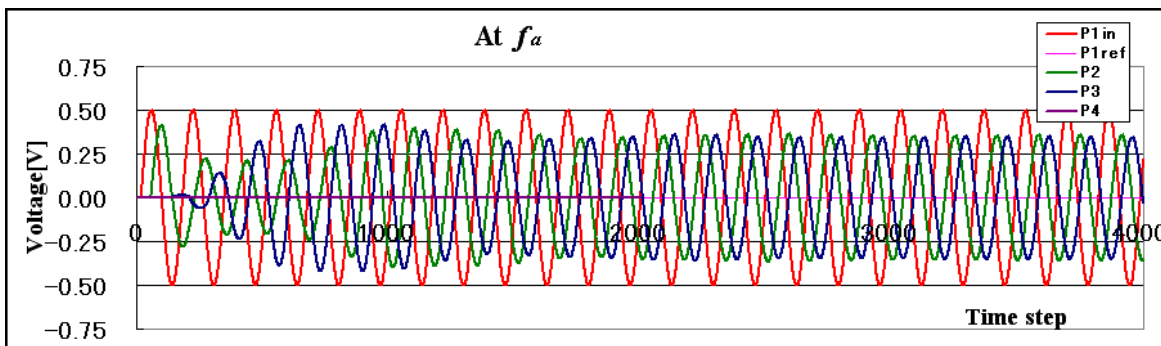


Figure 12. Variation of the instantaneous voltage and current distributions on the traveling-wave triple-loop directional filter after 3000 time steps at the center frequency. Red lines denote a snapshot of the plot.



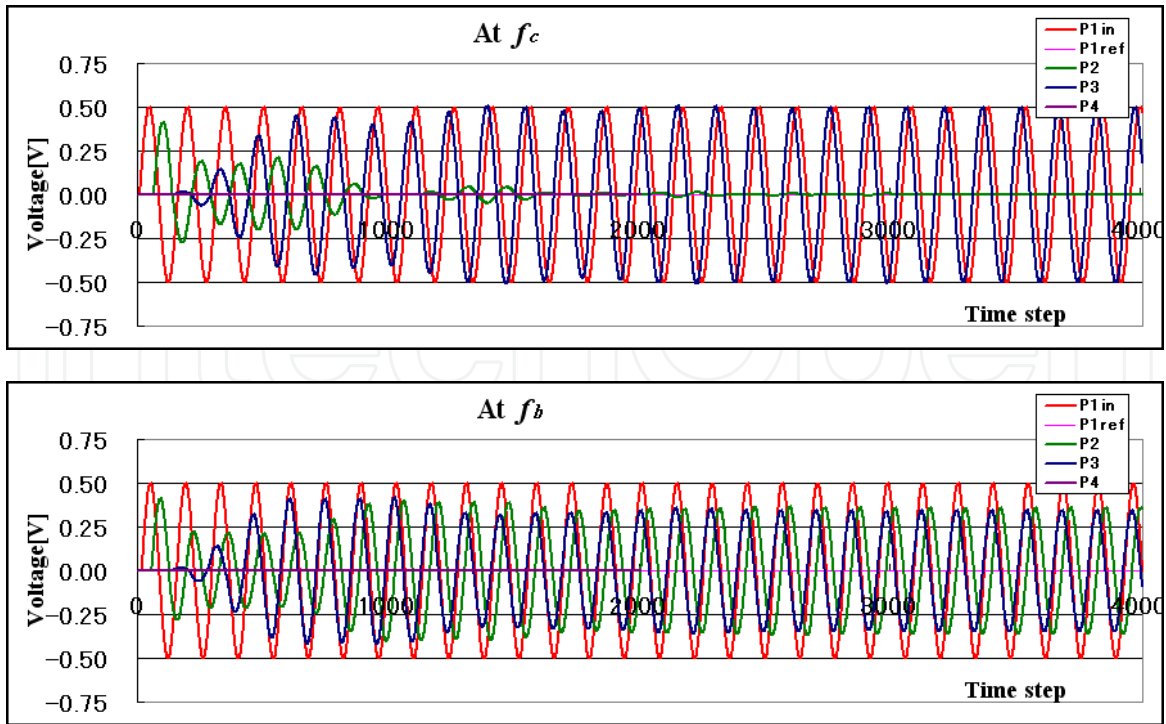


Figure 13. Input and output voltage waveforms of the traveling-wave triple-loop directional filter for f_a ($=1.72\text{GHz}$), f_c ($=1.875\text{GHz}$) and f_b ($=2.03\text{GHz}$) frequencies. (See Figure 16 (b))

4. Frequency responses

As an application of this method, it is shown that frequency responses are obtained from the transient responses by the fast Fourier transform technique. Using the input and output responses extracted from the transient pulse solutions, we obtain each voltage $V_{pn}(t)$ and current $I_{pn}(t)$ as the response quantities at port n . By using the FFT technique, S parameters for port 1 input of the coupler are given by

$$S_{n1} = \text{FFT}[V_{pn}(t)] / \text{FFT}[V_{in}(t)] \quad (15)$$

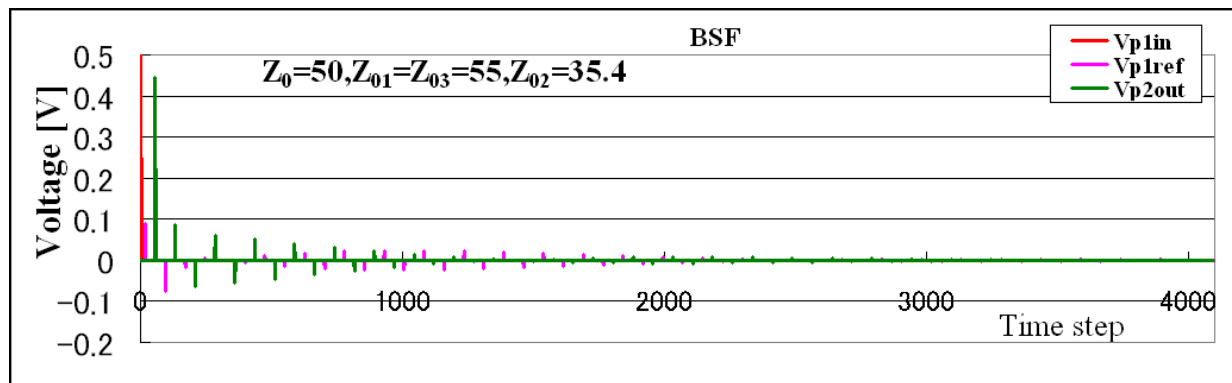
where $V_{in}(t) = (V_{p1}(t) + I_{p1}(t)Z_0)/2$ is the incident voltage at port 1. Then, the return loss S_{11} and insertion loss S_{21} are obtained. This simulation was carried out with a Gaussian pulse $e_i(t) = \exp(-((t-t_0)/\tau)^2)$ excitation, where t_0 is the initial delay time and τ is the pulse width parameter.

Figure 14 (a) illustrates the voltage pulse responses at each port for one loop resonator filter. Figure 14 (b) shows the return loss and insertion loss of the frequency characteristics, which has the characteristic of very sharp notch filter at the center frequency. The same line parameters in the previous section were used.

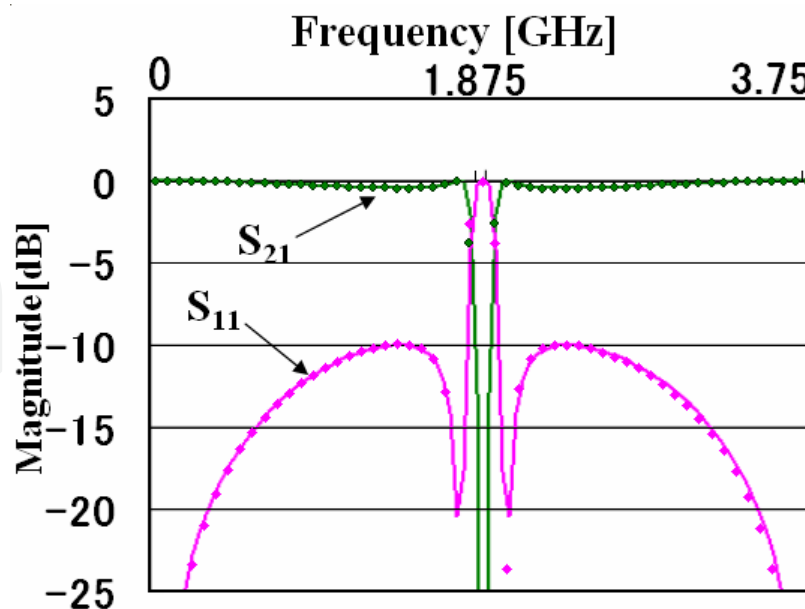
Figure 15 (a) illustrates the voltage pulse responses at each port for the traveling-wave double-loop 3-dB directional coupler. And, Figure 15 (b) shows the return loss and insertion loss of the frequency characteristics, which has the characteristic of band pass filter with 3dB coupling at the center frequency. Similarly, the result of the traveling-wave triple-loop

directional filter is shown in Figure 16. It can be seen that from the frequency response, the sharp skirt characteristics compared with double-loop resonators is obtained. The simulated results of the present method are in good agreement with those of S-NAP design software package [10].

Thus, by using the presented simulation tool, the circuit designers can efficiently obtain the design parameters to improve the properties of the ring resonator and traveling-wave loop directional filters in both the time and frequency domains. Also, by the visual expression of the solutions, the signal propagation can be make it easy to understand the operation characteristics on the microwave circuit components composed of the coupled transmission lines. Finally, the implemented program is of compact algorithm by the Visual BASIC language, and considerably saves CPU time.

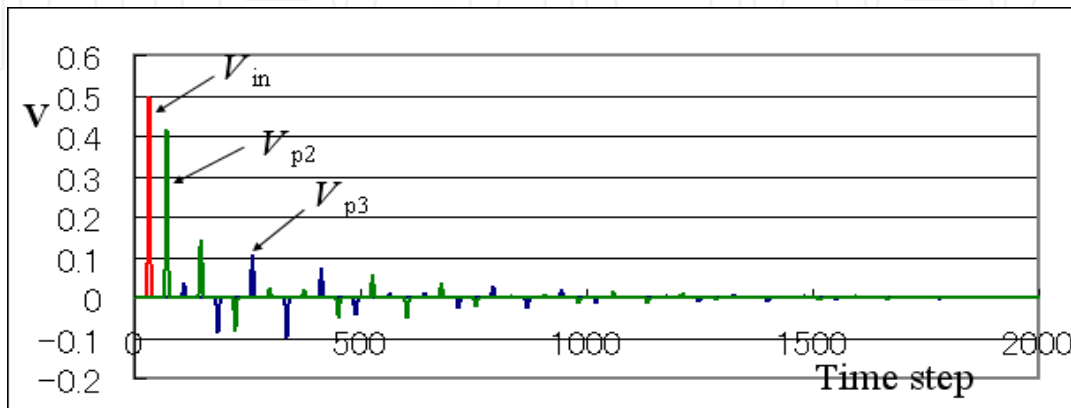


(a)

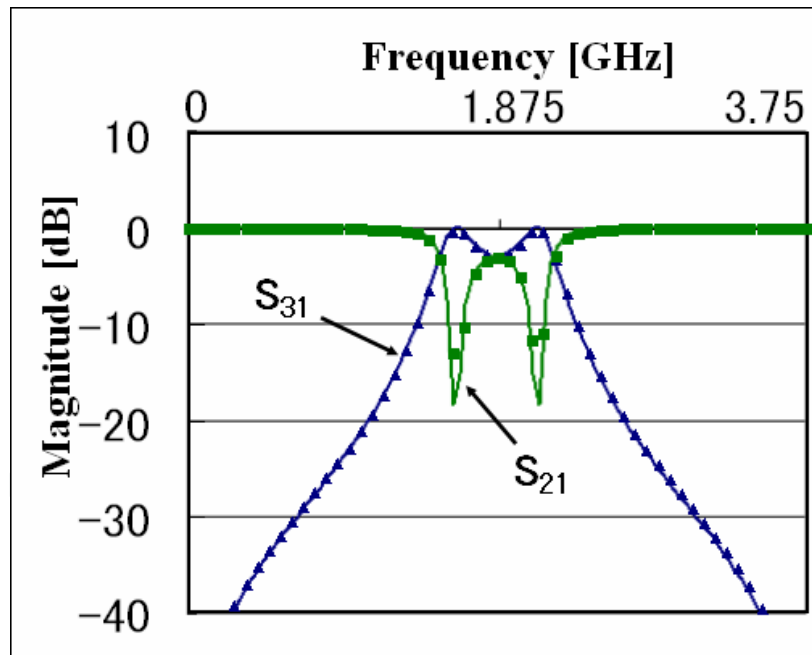


(b)

Figure 14. (a) Input and output voltage responses of the ring resonator BSF from 0 to 4000 time steps for a Gaussian excitation. (b) S-parameters by present method (dotted lines), and SNAP simulator (solid lines).



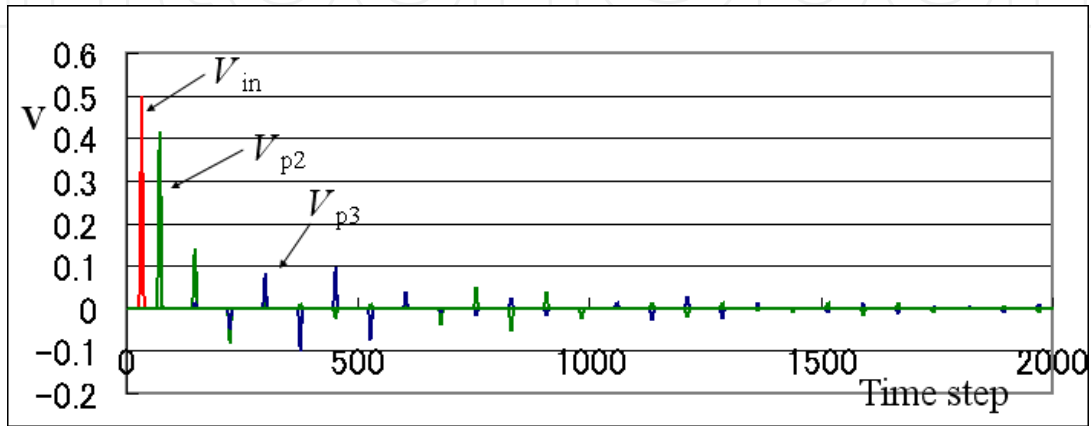
(a)



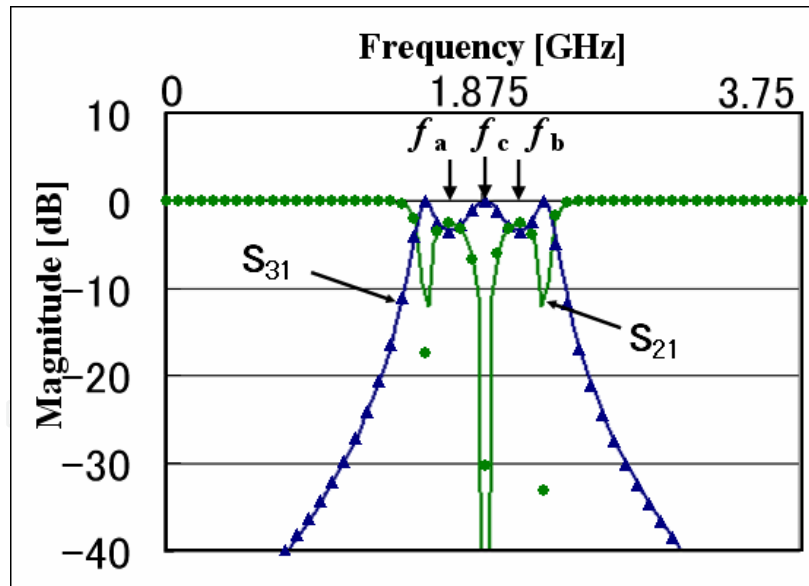
(b)

Figure 15. (a) Input and output responses of the traveling-wave double-loop directional coupler for a Gaussian pulse excitation. (b) S-parameters of this coupler: presented method (dotted lines), and SNAP simulator (solid lines).

IntechOpen



(a)



(b)

Figure 16. (a) Input and output responses of the traveling-wave triple-loop directional filter for a Gaussian pulse excitation. (b) S-parameters of this filter: presented method (dotted lines), and SNAP simulator (solid lines).

5. Conclusion

Visualizing the signal propagation in transmission line circuits is very important for understanding the operation mechanism of the circuit systems. It has been shown that the presented time domain simulation method can analyze and demonstrate the transient behaviors of the voltage and current waves of the ring resonator and traveling-wave loop directional filters by dynamic expression. Moreover, we have shown the frequency responses of the multi-loop coupled line filters by using the FFT technique. As a brief test tool, this method introduced the systematic mixed even and odd modes model for the part of parallel coupled lines is useful to confirm the operation characteristics of the circuit components consisted of loop resonator with coupled lines. This run can process on a small size PC system sufficiently.

Author details

Kazuhito Murakami
Computing Center, Kinki University, Japan

6. References

- [1] T. Itoh, et al, Numerical techniques for microwave and millimeter-wave passive structures, JOHN WILEY & SONS, 1989.
- [2] R. F. Harrington, Field computation by moment method, IEEE Press, 1993.
- [3] K. S. Yee, Numerical solutions of initial boundary value problems involving Maxwell's equations in isotropic media, IEEE Trans. Antennas & Propag., vol.AP-14, no.3, May 1966, pp.302-307.
- [4] A. Taflove and S. C. Hagness, Computational electrodynamics the Finite-Difference Time-Domain method, ARTECH HOUSE, MA, 2000.
- [5] G. Matthaei, L. Young and E.M.T. Jones, Directional, channel-separation filters and traveling-wave ring-resonators, in Microwave filters, impedance-matching networks, and coupling structures, Chapter 14, pp.843-887, ARTECH HOUSE, MA, 1980.
- [6] F. S. Coale, A traveling-wave directional filter, IRE Trans. on MTT, vol. 4, no.10, Oct. 1956, pp.256-260.
- [7] M. K. M. Sallich, G. Prigent, O. Pigaglio, and R. Crampagane, Quarter-wavelength side-coupled ring resonator for bandpass filters, IEEE Trans. Microwave Theory Tech., vol. MTT-56, no. 1, Jan. 2008, pp.156-162.
- [8] K. Murakami, and J. Ishii, Transient analysis of multi-section transmission line using modified central difference method (In Japanese), Trans. IEICE Vol.J78-A, May 1995, pp. 602-609.

- [9] K. Murakami, and S. Kitazawa, Transient responses of voltage and current on ring resonator and traveling-wave loop directional filters, in Proc. of APMC2010, pp. 1185-1188, Dec. 2010, Yokohama, Japan; 2010.
- [10] S-NAP Design user's manual, MEL Inc., 1998.

IntechOpen

IntechOpen